

Solvent-Induced Crystallization in Polyetherimide Thermoplastics and Their Carbon Fiber Composites

K. M. NELSON, J. C. SEFERIS,* and H. G. ZACHMANN¹

Polymeric Composites Laboratory, Department of Chemical Engineering, University of Washington, Seattle, Washington 98195, and ¹Institute of Technology and Macromolecular Chemistry, University of Hamburg, Hamburg, Germany

SYNOPSIS

Solvent-induced crystallization (SINC) was observed in a polyetherimide (PEI), a thermoplastic used as a matrix in carbon fiber composites. This observation was made using wide angle X-ray scattering (WAXS), differential scanning calorimetry (DSC), and optical microscopy. It was discovered that methylene chloride induces crystallization in the PEI by penetrating the surface and swelling the bulk polymer. Prepreg processed using *N*-methyl pyrrolidone (NMP) was also crystalline. Once processed above the crystalline melting point (T_m), no crystallinity in the sample was found, as the PEI did not crystallize from the melt. The observed crystallization of both the neat polymer and its carbon fiber prepreg was exclusively through a solvent-induced process, although it is likely that the mechanism through which crystallization occurs during solvent prepreg processing is different than the diffusion-controlled mechanism demonstrated with methylene chloride. A solvent prepregging process may involve a low molecular weight or monomer solution as well as other polymerization by products. Measurements using WAXS showed a maximum degree of crystallinity of 30%, as induced by methylene chloride. A value of 85 J/g for the heat of solvent-induced crystallization in the PEI was calculated from the DSC measurements.

INTRODUCTION

The use of solvents may be essential in the prepregging and the consolidation of thermoplastic based composites; however, the presence of a solvent in the matrix of a composite can have far-reaching effects on the structure and its resulting bulk properties. For example, upon absorption of a low molecular weight penetrant, the polymer swells, resulting in cracks, cavities, and sometimes crystallization, which may be a consequence of the solvent process of the matrix in the prepreg.¹ Indeed, one advantage semicrystalline thermoplastic matrix

composites have over their amorphous matrix counterpart is the intrinsic solvent resistance of the crystalline phase.

Solvents have been widely utilized in the impregnation of high T_g thermoplastics as well as in thermosets. In the lamination of a prepreg into a composite, it may be beneficial or necessary to have a certain amount of solvent present in order to enhance bond line formation. In this study, a polyetherimide (PEI) was found to crystallize in the presence of a solvent commonly used in prepreg manufacturing processes.

Crystallinity can be described as the ordering of the polymer chains to achieve a thermodynamically favored lower entropy configuration. Semicrystalline polymers may increase in crystallinity due to solvent plasticization and swelling. This phenomenon has been specifically described by Stober and Seferis for

* To whom correspondence should be addressed.

poly(ether ether ketone) (PEEK), which is used as a composite matrix system.^{2,3}

The degree of crystallinity is usually defined as the fraction of crystalline phase in the bulk polymer. Semicrystalline polymers have been traditionally modeled as two-phase systems made up of crystalline and noncrystalline regions. For semicrystalline polymers, the degree of crystallinity, size of crystals, and orientation of the crystalline and noncrystalline regions form the basis for the microstructure of the polymer. This microstructure has been successfully correlated to the bulk polymer properties.⁴

Transport of low molecular weight fluids into a semicrystalline thermoplastic takes place almost exclusively in the amorphous phase. When the crystallinity increases by additional crystallization of the amorphous phase as a result of solvent penetration, the phenomenon has been defined as solvent-induced crystallization (SINC). SINC has been observed in poly(ethylene terephthalate) (PET), polycarbonate (PC), Poly(ether ether ketone) (PEEK), and of interest here, polyetherimide (PEI).^{1,5-7} Solvent-induced crystallization may be accompanied by other penetrant associated structural changes, such as microcracking, crazing, and cavitation. In this study we have focused primarily in quantifying solvent-induced crystallization in both neat PEI and its carbon-reinforced composites.

THEORY

As a solvent penetrates the surface of a thermoplastic polymer, the polymer swells, producing a rubbery surface layer separated from the bulk by a distinct front. Often, solvent-induced crystallization accompanies the swelling front as seen in poly(ethylene terephthalate) (PET).⁸ In the particular case where crystallization accompanies the diffusion front, Durning and Russell developed a mathematical model which describes the diffusion of a penetrant into the polymer.^{9,10} One phenomenon associated with solvent-induced crystallization is sorption overshoot, where the fully swollen polymer exudes solvent in response to induced crystallization.¹¹

Zachmann was the first to describe the kinetics of PET crystallization by SINC.¹² He found that crystallization kinetics are dependent upon the comparative rates of diffusion and crystallization. X-ray diffraction is often the preferred method of studying crystallization. An X-ray scattering pattern

of a semicrystalline polymer produces crystalline peaks superimposed upon an amorphous halo. In a carbon fiber reinforced composite, the X-ray scattering of the carbon fibers is also superimposed onto the scattering of the crystals. The degree of crystallinity is measured by comparing the relative intensity of the crystalline and amorphous scattering curves.

Before any calculations for crystallinity are made, the data are corrected for air scattering, absorption, polarization, and incoherent scattering.¹³ Data reduction uses the definition of reciprocal lattice space

$$s = |\mathbf{s}| = \frac{2 \sin \theta}{\lambda} \quad (1)$$

where λ is the wave length of radiation (CuK α = 1.54 Å), $|\mathbf{s}|$ is the magnitude of the reciprocal lattice vector \mathbf{s} , and θ is the angle of incident radiation. At any point in reciprocal space, if $I(s)$ is the intensity of the coherent X-ray scatter, and $I_c(s)$ is the intensity of the crystalline peaks, then the integral of crystalline peaks over all reciprocal lattice space squared compared to the integral of the total scattering curve is, to a good approximation, the weight fraction crystallinity^{14,15}

$$X_c = \frac{\int_0^\infty s^2 I_c(s) ds}{\int_0^\infty s^2 I(s) ds} \quad (2)$$

This calculation (2) produces a result which is generally slightly smaller than the true crystalline fraction. A portion of the scattered intensity from the crystalline fraction is lost from the peaks due to atomic thermal vibrations and lattice imperfections. Although this may be corrected using the Ruland method, which is not the focus of this study, our reported crystallinity values calculated from X-ray data may be slightly underestimated.¹⁶

Absorption of X-rays by a material is governed by the linear absorption coefficient for the material and the thickness of the material, described by the differential equation

$$\frac{dI}{dx} = -I\mu \quad (3)$$

where x is the thickness, I is the intensity of the X-ray beam, and μ is the linear absorption coefficient. The value of the linear absorption coefficient can be

approximated from tabulated values of the constituent atoms. In this study, the absorption coefficient for the PEI was measured experimentally from eq. (3) as $\mu = 0.68 \pm 0.03$ 1/mm.

By integration of the DSC melting endotherm, the heat of crystallization of the particular sample can be evaluated. When compared to the degree of crystallinity calculated using WAXS, the heat of crystallization of 100% crystallized PEI can be calculated by

$$\Delta H_f = \frac{\Delta H_m}{(1 - m_f) X_c} \quad (4)$$

where ΔH_f is the heat of crystallization of 100% crystallized PEI, ΔH_m is the DSC measured heat of crystallization, m_f is the total fiber fraction by mass, and X_c is the crystallinity fraction. The degree of crystallinity of any particular PEI sample can be calculated from DSC data by application of this equation and the constant ΔH_f .

EXPERIMENTAL

The polyetherimide-carbon fiber prepreg used in this study was produced by American Cyanamid Co. under the trade name of CYPAC X7005.¹⁷ The PEI matrix is based on General Electric's Ultem family of resins whose typical chemical structure is shown in Figure 1.

A carbon fiber fabric was used as the reinforcement in the PEI prepreg, giving the orientation of the fibers as 0/90°, indicative of the fabric pattern. The carbon fiber fabric was a 3000 filament tow designated 3K70P-AS-4. Additional information about the PEI prepreg and composites may be found in the literature.¹⁸

X-ray diffraction measurements were performed with a Siemen's diffractometer (D500) using CuK α radiation (1.54 Å) and a Nickel filter. All scattering measurements were performed in transmission. Scattering was measured at angles of 2θ ranging from 5 to 70°. To measure the absorption coefficient and the scattering of neat carbon fibers, the matrix material from the prepreg was digested using sulfuric acid. Once the polymeric matrix was dissolved, the fibers remained in their original orientation and quantity, allowing for direct X-ray measurements.

Differential scanning calorimetry (DSC), was performed on a Du Pont instrument, Model 912, interfaced to a Model 2000 TA controller. Isothermal heat treating of the samples was done in the DSC

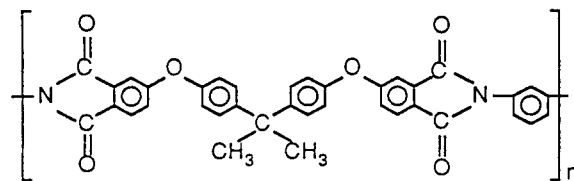


Figure 1 Representative chemical structure of polyetherimide thermoplastics.

cell for a period of 1 h, at which time no data were recorded. The sample was cooled to ambient temperature and then heated at 10°C/min to 375°C to generate the DSC trace. All DSC runs were performed in a nitrogen atmosphere.

Optical microscopy was performed using a Nikon microscope. Samples were sectioned, mounted, and polished. Cross-polarized light was used to highlight the crystalline portion in the cross section.

RESULTS AND DISCUSSION

Solvent-Induced Crystallization (SINC)

When a polyetherimide film was placed in a bath of methylene chloride, the polymer began to swell. A thin white layer, visible to the naked eye, formed immediately on the polymer surface, and the sample turned opaque as crystallization began. A sharp crystallization front formed and moved towards the center of the sample following the diffusion front. When the two crystallization fronts (one from each side) met, the polymer continued to absorb solvent until the saturation point was reached.

In thicker samples, the depth of crystallization was examined using optical microscopy and polarized light. Figure 2 shows the boundary between the crystallized phase and the amorphous phase. Cracking was observed during desorption as the crystalline phase contracted above the underlying amorphous phase, which had a larger specific volume. The cracks propagated along the surface, similar to mud drying on a lake bed. Whenever a propagating crack intersected another crack, a T shape was formed. Figure 3 shows the intersection of two cracks on the surface of a thick film. The observed angle of the crack intersection was always 90°, which may be a result of the release of the internal stress component perpendicular to the crack length.

Upon initial contact of the PEI with the methylene chloride, the surface of the PEI became white. A similar phenomenon has been reported in the literature and attributed to surface cavitation which

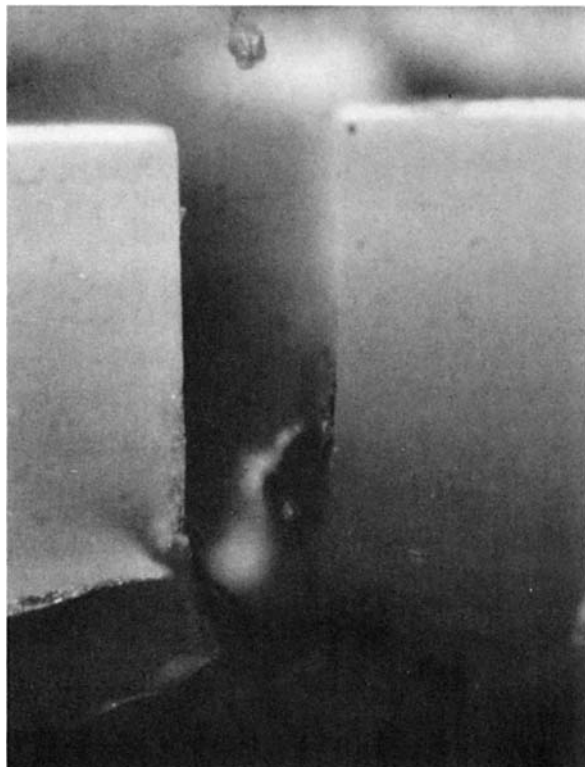


Figure 2 Photomicrograph in cross-polarized light, showing induced crystallization in the polyetherimide. Three distinct regions were observed. The white layer at top is a crystalline region with surface cavitation. The crack propagated through the crystalline region, shown in light grey, and stopped at the amorphous interface, shown in black at the bottom.

occurs during initial rapid absorption of the solvent.¹⁹ When solvent rapidly penetrates the surface, crystal nucleation occurs in the swollen areas, and crystal growth proceeds radially from the nucleation sites. Associated with each crystal and with the entire crystallization process is a contraction and a net decrease in specific volume. This is accompanied by an exclusion of solvent during additional crystallization. The amorphous region becomes supersaturated with solvent, inducing phase separation and the formation of microcavities. The rate of solvent uptake decreases as the front moves beyond the surface where cavitation does not occur.

Wide Angle X-Ray Scattering

An amorphous halo is a manifestation of the statistical distribution of distances between scattering centers, producing in a sense, a type of short-range order. The result is a broad interference pattern representative of the most probable distance be-

tween scattering centers. Figure 4 shows the amorphous halo of the PEI system quenched from a melt. A similar sample slowly cooled from a melt produces an amorphous halo identical to that of the quenched sample, as was expected for an amorphous polymer. The PEI system, as with other amorphous systems had the same microstructure regardless of the cooling rate.

Crystallization was evident in the WAXS of the PEI prepreg which was processed using a solvent. Figure 5 shows the WAXS scan for the PEI prepreg showing several sharp well-defined crystalline peaks, and two broad peaks resulting from carbon fiber scattering. The degree of crystallinity of the prepreg was calculated to be 16% by weight. The orientation of the carbon fibers in the prepreg was 0/90°, typical for woven fabric reinforcement, the azimuthal angle being 0°, with fibers aligned horizontally and vertically.

Correcting the prepreg scattering curve for the presence of carbon fibers resulted in a curve representative of the randomly oriented semicrystalline

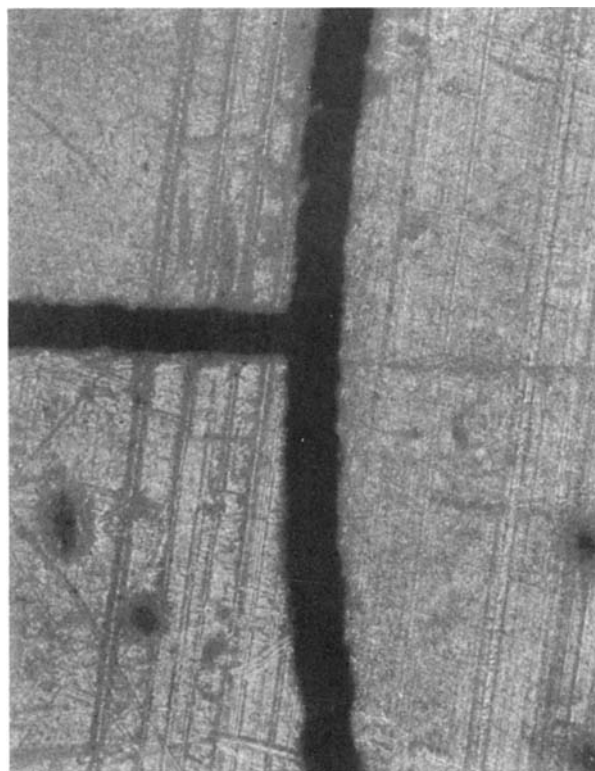


Figure 3 Low magnification (160 \times) view of the PEI surface after solvent-induced crystallization and desorption of methylene chloride. Cracks propagated across the surface and intersected each other at 90° angles, as internal stresses were relaxed perpendicular to the direction of crack propagation.

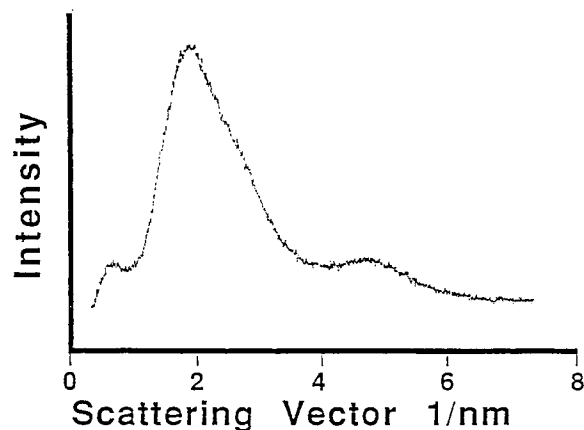


Figure 4 Wide angle X-ray scan of neat PEI resin showing the amorphous halo. The PEI had an identical halo regardless of cooling rate, indicating that the PEI will not crystallize from the melt. The PEI was always amorphous when heated above 310°C, or when not exposed to a solvent.

structure of the PEI matrix. Figure 6 schematically illustrates the process of subtracting the carbon fiber data from PEI prepreg data, resulting in a fiber-free diffraction pattern of the PEI matrix. The carbon fibers in a prepreg or composite produce an orientation effect which is evident when examining scans at different azimuthal angles. The azimuthal angle is the angle of rotation of the sample within the plane defined by the sample. In comparing Figure 5 with Figure 6, the broad peaks attributed to carbon fiber scattering have shifted with respect to a 45° change in the azimuthal angle.

Neat PEI resin exposed to methylene chloride for a period of 4 h became 30% crystalline, as can be seen in Figure 7. The PEI prepreg processed by solvent impregnation (*N*-methyl pyrrolidone) was 16% crystalline. It was observed that, by heating the PEI above its crystalline melting point, any history of its having been crystalline was removed. Upon cooling, the PEI remained noncrystalline, regardless of the cooling rate. Thus, this PEI will not crystallize from a melt. Table I summarizes the calculated crystallinity values for the different PEI samples examined.

If the PEI prepreg is processed above the crystalline melting point, the processed laminate will be amorphous and will remain amorphous unless exposed to a solvent. This phenomenon was directly observed by differential scanning calorimetry (DSC). Figure 8 shows the DSC thermogram of a prepreg processed with NMP, showing a glass transition at 225°C and the onset of melting at 280°C. When a semicrystalline PEI sample was heated

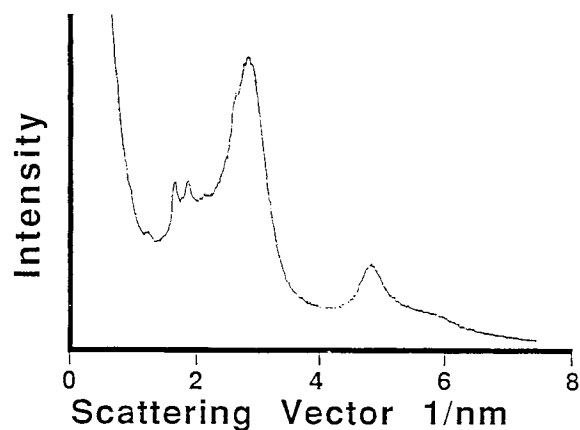


Figure 5 Wide angle X-ray scan of prepreg impregnated with PEI using NMP. Fibers were oriented 0 and 90° due to the fabric. The broad diffraction peaks at $s \sim 2.9$ and $s \sim 4.8$ are attributed to carbon fiber scattering. The more prominent crystallization peaks are observed between $s = 1.0$ and $s = 2.3$. The mass fraction crystallinity in this sample was calculated at 16%. WAXS experiments were performed in transmission.

above the melt temperature, followed by cooling below the glass transition, and subsequently heated, the DSC trace showed an enhanced glass transition

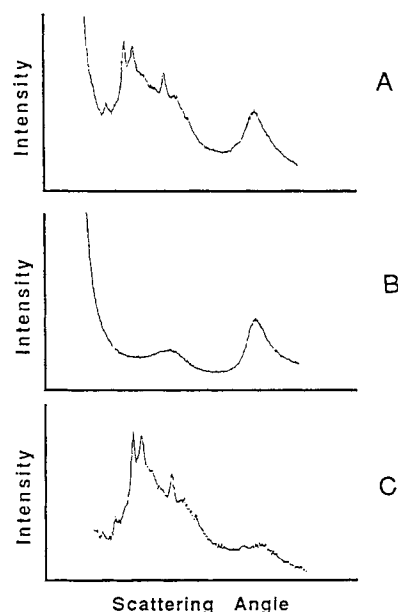


Figure 6 The process of subtracting carbon fiber WAXS data (B), from that of a prepreg (A), to yield PEI matrix data on a fiber free basis (C). The WAXS data for the carbon fibers were generated using resin-digested prepreg samples. The degree of crystallinity was then calculated by fitting the amorphous halo to the crystalline curve and integrating the relative contributions, as shown by eq. (2) in the text.

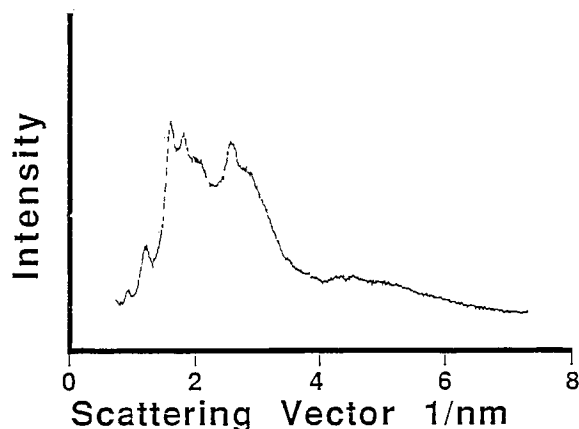


Figure 7 Methylene-chloride-induced crystallization in the PEI thermoplastic shown by WAXS. This thin sample was exposed to methylene chloride for a period of 4 h and then allowed to dry for an extended length of time. The mass fraction crystallinity in this sample was calculated at 30%. WAXS experiments were performed in transmission.

and no crystalline melting endotherm. This PEI will only crystallize through a solvent-induced process, and will not crystallize from the melt.

The crystallinity of semicrystalline polymers can be conveniently examined using DSC. The heat of melting may be calculated from the area of the endotherm shown by the DSC traces (Fig. 8). Using a degree of crystallinity of 16%, as determined from WAXS, the specific heat of melting was calculated from eq. (4) as 85 J/g.

By heating semicrystalline polymers below the melt temperature but above the glass transition temperature, the crystals may become more perfect and the degree of crystallinity may be increased through annealing. For this particular PEI system, however, annealing did not increase the crystallinity, as shown by the DSC thermogram of Figure 9. When solvent-crystallized PEI was heated at or below 270°C, there was no increase in crystallinity as shown by the DSC thermogram. When heated at 280°C, the melt temperature increased to 290°C and there was a slight decrease in crystallinity. For every 10°C increase in heat treating temperature above 270°C, there was a significant decrease in crystallinity. When the sample was heat treated at 310 °C, no crystallinity was observed.

Heating did not increase the crystallinity of the PEI as in traditional melt crystallizable polymers. However, by heating solvent crystallized PEI close to its melting point of 280°C, a portion of its crystalline region was melted. The amount of crystals that was melted was determined by how much above

T_m the sample was heated. Once heated above 310°C, the sample became amorphous and remained amorphous upon cooling.

Solvent-induced crystallization represents one of several documented processing-induced morphological changes in thermoplastic polymers and their composites. Although more attention has been focused on the effects of cooling rate on the crystallinity in semicrystalline matrix polymers, solvent-induced crystallization may also affect the processability of composite systems.²⁰ This work reports the first measurement of solvent-induced crystallization in a polyetherimide polymer, and its existence in a solvent processed carbon fiber reinforced prepreg before thermal consolidation into a laminate.

CONCLUSIONS

Solvent-induced crystallization was observed in a polyetherimide, both in its neat form and as a matrix in a carbon fiber reinforced prepreg. Measurements using WAXS indicated the maximum degree of crystallization of an initially amorphous PEI sample was 30% when exposed to methylene chloride for an extended length of time. Carbon fiber fabric prepreg which had been processed with NMP was found to be 16% crystalline. However, this may change, depending on the prepregging conditions. The observed crystallization of both the neat polymer and its carbon fiber prepreg was exclusively through a solvent-induced process. However, the mechanism through which crystallization occurs during solvent prepreg processing may be different than the diffusion-controlled mechanism demonstrated with methylene chloride, especially if reacting monomers are used as the starting material. In any case, the

Table I Crystallinity Determined by WAXS of PEI under Different Processing Conditions

1. Neat PEI quenched from melt	0%
2. Neat PEI slow cooled from melt	0%
3. NMP processed PEI prepreg	16%
4. 325°C Heat treated, NMP processed PEI prepreg	0%
5. 240°C Annealed, NMP processed PEI prepreg	17%
6. 3 Ply laminate of NMP processed PEI prepreg, quenched cooled	0%
7. 3 Ply laminate of NMP processed PEI prepreg, quenched	0%
8. MeCl ₂ -treated PEI	30%
9. NMP-treated PEI	< 5%

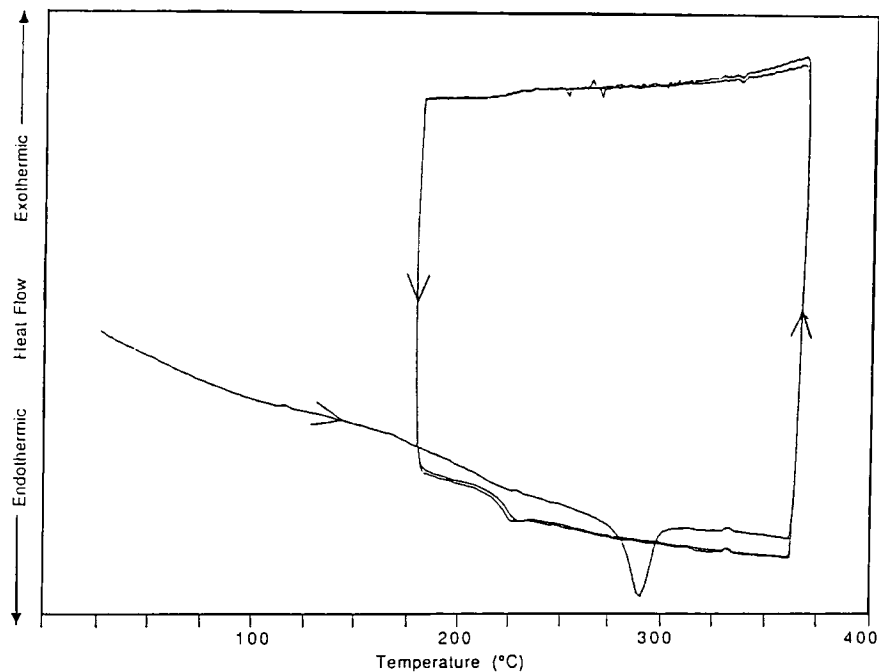


Figure 8 DSC of heating cycles PEI/CF prepreg processed using NMP. Arrows indicate direction (heating/cooling) of cycle. In the first heating cycle, initiated from 25°C, a subtle glass transition and a prominent crystalline melting endotherm at 275°C were observed. On the second and subsequent heating cycles, the melting endotherm was eliminated, and the glass transition was prominently exhibited at 220°C. Heating rate was 10°C/min.

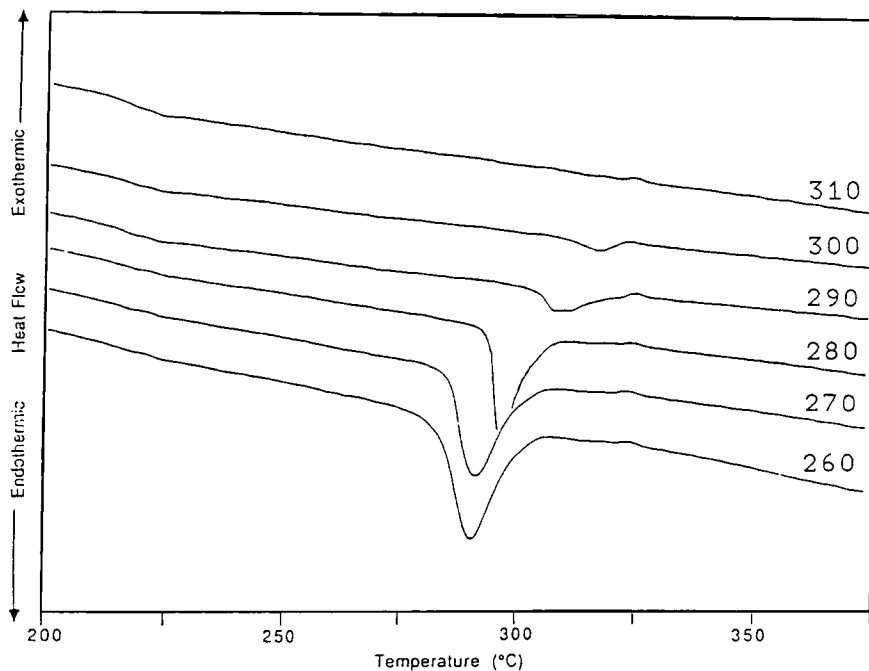


Figure 9 Isothermal heat treatment of PEI/CF prepreg processed using NMP. Samples were held isothermally for 1 h, cooled, and then heated at 10°C/min to produce the DSC trace. Six isothermal temperatures are shown ranging from 10°C below T_m to 40°C above T_m . Heat treating reduced crystallinity and shifted T_m to higher temperature as shown by the melting endotherms.

PEI did not crystallize from the melt. The heat of crystallization for this particular solvent crystallizable polyetherimide was calculated at 85 J/g, using DSC data. Solvent-induced crystallization (SINC) has been observed in other polymers, PET, PC, and etc., as well. The degree of crystallization depends on the type of solvent, length of exposure, and other processing conditions. This work has shown that the PEI examined behaves quite similar to what has been reported in the literature for the other polymers. Finally, it should be noted that, although solvent processable PEI prepreg may be crystalline, it will result in an amorphous laminate if the processing temperature exceeds the melting point of the solvent induced crystalline phase.

The authors would like to express appreciation to Dr. S. L. Peake of American Cyanamid Co. and S. Rober, U. Koncke, and C. Schipp of the Institute of Technology and Macromolecular Chemistry, University of Hamburg, Germany, for helpful discussions. Financial assistance for this work was provided by American Cyanamid Co., through project support to the Polymeric Composites Laboratory at the University of Washington (1986–1989). The Alexander von Humboldt Foundation and the University of Hamburg are gratefully acknowledged for their support to K. M. Nelson and J. C. Seferis during their work in Germany.

REFERENCES

1. K. M. Nelson, J. C. Seferis, and H. G. Zachmann, *34th Int. SAMPE Symp. Proc.*, 69 (1989).
2. E. J. Stober, J. C. Seferis, and J. D. Keenan, *Polymer*, **25**, 1845 (1984).
3. E. J. Stober and J. C. Seferis, *Polym. Eng. Sci.*, **28**(9), 634 (1988).
4. J. C. Seferis and R. J. Samuels, *Polym. Eng. Sci.*, **19**(14), 975 (1979).
5. J. Wang, A. J. DiBenedetto, J. F. Johnson, S. J. Huang, and J. L. Cercena, *Polymer*, **30**, 718 (1989).
6. N. C. Thomas and A. H. Windel, *Polymer*, **23**, 529 (1982).
7. N. C. Thomas and A. H. Windel, *Polymer*, **21**, 613 (1980).
8. P. J. Makarewicz and G. L. Wilkes, *J. Polym. Sci.*, **16**, 1529 (1978).
9. C. J. Durning and W. B. Russell, *Polymer*, **26**, 131 (1985).
10. R. O. Johnson and E. O. Teutsch, *Polym. Compos.* **4**(3), 162 (1983).
11. R. Ware, S. Tirtowidjojo, and J. Cohen, *J. Appl. Polym. Sci.*, **26**, 2975 (1981).
12. H. G. Zachmann and G. Konrad, *Makromol. Chem.*, **118**, 189 (1968).
13. B. R. Coxon, MS thesis, Department of Chemical Engineering, University of Washington, Seattle, WA, 1988.
14. W. Ruland, *Acta Cryst.*, **14**, 1180 (1961).
15. L. E. Alexander, *X-Ray Diffraction Methods in Polymer Science*, Kreiger, 1979.
16. W. Ruland, *Polymer*, **5**, 89 (1964).
17. S. L. Peake, A. Maranci, and D. Megna, *34th Int. SAMPE Symp. Proc.*, 1235 (1989).
18. S. L. Peake, A. Maranci, and E. Strum, *32nd Int. SAMPE Symp. Proc.*, 421 (1987).
19. C. J. Durning, L. Rubinfeld, W. B. Russell, and H. D. Weigmann, *J. Polym. Sci., Polym. Phys. Ed.*, **24**, 1341 (1986).
20. C. N. Velisaris and J. C. Seferis, *Polym. Eng. Sci.*, **26**(12), 1574 (1986).

Received February 8, 1990

Accepted May 14, 1990